Molecular Genetics & Genomic Medicine

WILEY

Molecular Genetics & Genomic Medicine
Open Access

REVIEW ARTICLE OPEN ACCESS

Expanding the Clinical and Genetic Spectrum of Mitochondrial Short-Chain Enoyl-CoA Hydratase 1 Deficiency: Insights From Two Unrelated Chinese Families

Jihua Wu[1] | Xuehui Hu[1] | Zhongli Zhao[1] | Zhen Zhao[2] | Bin Yang[1]

[1]Department of Neurology, Anhui Provincial Children's Hospital, Hefei, China | [2]Department of Imaging, Anhui Provincial Children's Hospital, Hefei, China

Correspondence: Bin Yang (0111yangbin@sina.com)

Received: 7 August 2024 | **Revised:** 8 February 2025 | **Accepted:** 26 March 2025

Funding: This work was supported by the Natural Science Foundation of Anhui Province (Grant 2108085MH268).

Keywords: developmental delay | *ECHS1* gene | Enoyl-CoA hydratase | metabolic acidosis

ABSTRACT

Background: Mitochondrial short-chain enoyl-CoA hydratase 1 deficiency (ECHS1D) is a rare autosomal recessive disorder affecting valine metabolism, with clinical severity ranging from neonatal death to survival into adulthood. Despite advances in understanding ECHS1D, the genetic basis remains underexplored, particularly in underrepresented populations.

Methods: This study aimed to investigate the clinical and genetic characteristics of ECHS1D in two unrelated Chinese families and identify novel pathogenic variants. Clinical and genetic data were collected, and whole-genome sequencing was performed to identify pathogenic variants in the *ECHS1* gene.

Results: The first proband, a 15-month-old girl, presented with developmental delays and metabolic acidosis, with an MRI revealing abnormal signals in the basal ganglia. The second proband, a 6.5-year-old girl with movement-induced dystonia, exhibited lethargy following recurrent fever and vomiting, with similar MRI findings. Genetic testing identified novel compound heterozygous variants: c.759_762del (p.Gly255Valfs*21) and c.489G>A (p.Pro163=) in Proband 1 and c.518C>T (p.Ala173Val) and c.244G>A (p.Val82Met) in Proband 2. The c.759_762del (p.Gly255Valfs21) variant, identified for the first time, likely results in severe symptoms due to a loss of normal function.

Conclusion: These findings expand the *ECHS1* mutational spectrum and emphasize the importance of genetic testing for early diagnosis and personalized management of ECHS1D. Interventions such as dietary valine restriction and the avoidance of triggering factors may improve clinical outcomes, while further research is needed to explore targeted therapeutic strategies.

1 | Introduction

Mitochondrial short-chain enoyl-CoA hydratase 1 deficiency (ECHS1D; OMIM # 616277) is a rare and severe autosomal recessive metabolic disorder caused by variations in the *ECHS1* gene (OMIM*602292). This encodes a crucial mitochondrial enzyme involved in fatty acid β-oxidation and branched-chain amino acid metabolism (Peters et al. 2014). Variations in *ECHS1* impair normal energy production, leading to the accumulation of toxic metabolites that result in a range of clinical symptoms (François-Heude et al. 2022). ECHS1D typically manifests during infancy, with a high fatality rate often

resulting in death during childhood. The clinical features include developmental delay, neurodegenerative regression, hyperlactatemia, and characteristic basal ganglia abnormalities (Peters et al. 2014).

Due to its heterogeneous clinical presentation and lack of specific diagnostic markers, ECHS1 deficiency (ECHS1D) is frequently overlooked in the differential diagnosis of mitochondrial disorders, particularly those associated with Leigh syndrome. Leigh syndrome is characterized by defective oxidative phosphorylation (OXPHOS), and the loss of OXPHOS function in some ECHS1D patients suggests that ECHS1 enzyme activity may play a critical role in the assembly and stability of OXPHOS protein complexes (Burgin et al. 2023). Precise diagnosis is essential for appropriate counseling and treatment, including early intervention and dietary management targeting branched-chain amino acid metabolism to alleviate symptoms and improve the quality of life for affected individuals (Bernhardt et al. 2024).

First described as a fatal form of Leigh syndrome in 2014, ECHS1D has been reported in approximately 85 patients worldwide. However, reports from China remain limited, highlighting a critical knowledge gap (Balasubramaniam et al. 2017; Yang et al. 2022). This study provides a retrospective analysis of the clinical and genetic profiles of two unrelated Chinese families with ECHS1D and includes a comprehensive literature review. This study aimed to improve awareness and diagnostic accuracy for ECHS1D, facilitating better support and treatment for affected families. By identifying novel compound heterozygous variants of the *ECHS1* gene and emphasizing the importance of early diagnosis and intervention, this research offers valuable insights into the management and understanding of ECHS1D.

2 | Participants and Methods

2.1 | Ethical Compliance

Clinical data from two patients diagnosed with ECHS1D were collected at the Department of Neurology, Anhui Provincial Children's Hospital, in 2023. This study was approved by the Ethics Committee of Anhui Children's Hospital, and informed consent was obtained from the patients' guardians. Peripheral blood samples from both the patients and their parents were sent to the Beijing Chigene Translational Medicine Research Center Co. Ltd. for whole-genome sequencing analysis.

2.2 | Sample Collection

Genomic DNA was extracted from peripheral blood using the Blood Genome Column Medium Extraction Kit (Kangweishiji, China) in accordance with the manufacturer's protocol. Trio-whole-genome sequencing (trio-WGS) was performed on these DNA samples using the DNBSEQ-T7 platform (MGI, China). Genomic DNA was randomly fragmented using an ultrasound apparatus, and fragments of approximately 300 base pairs (bp) were selected for sequencing. WGS libraries were prepared with the MGIEasy Universal DNA Library Preparation Kit (BGI, China), following the manufacturer's instructions.

2.3 | Bioinformatics Analysis

Raw sequencing reads were processed using fastp to trim adapters and remove low-quality reads. Paired-end reads were then aligned to the human reference genome (GRCh37/hg19) using the Burrows-Wheeler Aligner (BWA v0.7.10). Variant calling and annotation were carried out using the Genome Analysis Toolkit (GATK v3.5), Picard (v1.128), and ANNOVAR. High-quality nucleotide polymorphisms (SNPs) and insertions/deletions (Indels) were identified based on stringent sequence depth and variant quality metrics. High-quality nucleotide polymorphisms (SNPs) and insertions/deletions (Indels) were identified based on stringent sequence depth and variant quality metrics. The average sequencing depth for the WGS samples was no less than 25X, with a Q30 score exceeding 85%, and coverage of 10X or greater was achieved for at least 94% of the genome. The total depth of the selected variant was $> 10\times$, the depth of the variant was $> 5\times$, and the variant frequency was > 0.3.

Minor allele frequencies (MAFs) were annotated using databases such as 1000 Genomes, Exome Aggregation Consortium (ExAC), NHLBI Exome Sequencing Project (ESP), dbSNP, and the Genome Aggregation Database (gnomAD) through the Chigene-developed online system (www.chigene.org). Pathogenicity assessments for gene variants were conducted according to ACMG guidelines and supported by bioinformatics predictions from tools such as MutationTaster, SIFT, Provean, M-Cap, Revel, and PolyPhen-2. Functional changes in splice sites were predicted using MaxEntScan, dbscSNV, and GTAG software packages. Candidate pathogenic variants were validated by Sanger sequencing in both probands and their parents to ensure accuracy and reliability (Table S1). The HGMD and ClinVar databases were consulted to confirm whether the identified variants had been previously documented.

3 | Results

3.1 | Clinical Findings of the Family 1

Proband 1 (Figure 1:II-2), a 15-month-old female, was admitted to the Rehabilitation Department of Anhui Children's Hospital on August 7, 2023, due to an inability to walk independently. Upon admission, she was unable to stand unsupported, exhibited limited speech consisting of monosyllabic and reduplicated words, failed to distinguish between relatives and strangers, and demonstrated poor cognitive function and comprehension. She was readmitted on September 24, 2023, with a one-day history of vomiting and a half-day history of fever. On physical examination, she was conscious but lethargic, with unstable head posture, grade VI muscle strength in the extremities, low muscle tone, and weakened tendon reflexes. Her body length was 82 cm (P90), and her weight was 10 kg (P50).

The patient was the second child born full-term via natural delivery, with a birth weight of 3850 g. There was no history of birth asphyxia or hypoxia. Family history revealed a healthy older brother and a 5-month-old younger sister (Figure 1:II-3)

who presented with hypotonia and feeding difficulties but normal brain MRI findings. The parents were healthy, unrelated, and reported no family history of genetic disorders. Auxiliary examinations, including routine blood tests, liver and kidney function tests, and assessments of electrolytes, lactate, blood ammonia, ceruloplasmin, and homocysteine levels, were unremarkable. However, her CO_2 binding capacity was initially reduced to 6.5 mmol/L (normal range 22–28 mmol/L), which improved to 25.5 mmol/L after 3 days of treatment. Blood gas analysis showed a mildly decreased pH value of 7.33 (normal range 7.35–7.45) and an HCO_{3-} level of 13.7 mmol/L (normal range 21.4–27.3 mmol/L). Cardiac, abdominal, and urinary tract ultrasonography revealed no abnormalities.

Blood tandem mass spectrometry indicated reduced valine levels (67.08 umol/L; normal range 80–300 umol/L), while other parameters were within normal limits. Urine organic acid analysis showed elevated levels of 2-methyl-2,3dihydroxybutyrate (2,3DH2MB) and S-(2-hydroxypropyl) cysteamine (SCPCM) (Table 1). Brain MRI conducted on August 30, 2023, showed symmetrical patchy abnormal signals in the bilateral basal ganglia, which persisted with diffusion restriction on a follow-up MRI performed on October 1, 2023 (Figure 2). The patient received treatment consisting of acid correction and mitochondrial supplementation therapy. However, her motor skills remained impaired, and no improvements were observed in cognitive function.

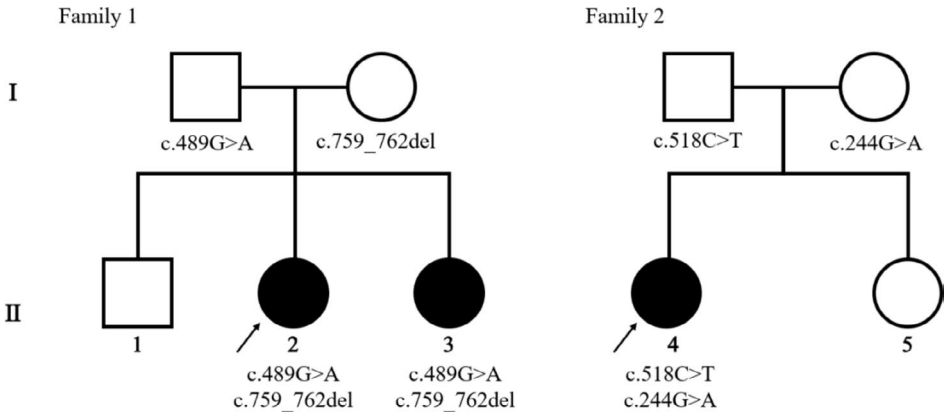

FIGURE 1 | ECHS1D pedigree diagram. The black arrow indicates the proband. Proband 1, her sister, and Proband 2 all carried compound heterozygous variants in the *ECHS1* gene, while their parents were heterozygous carriers of the respective variants.

TABLE 1 | Characteristics of metabolic markers in pedigree probands.

	Proband 1			Proband 2		
	Urine SCPCM	**Urine 2,3DH2MB**	**Blood C4OH**	**Urine SCPCM**	**Urine 2,3DH2MB**	**Blood C4OH**
Value	3.254↑	0.011↑	0.137	1.896↑	0.0114↑	0.146
Normal Range	< 0.624	< 0.0029	< 0.23	< 0.624	< 0.0029	< 0.23
Ratio	5.215	3.793	0.528	3.042	3.931	0.635

Note: SCPCM is S- (2-hydroxypropyl) cysteamine, 2,3DH2MB is 2,3-dihydroxy-2-methylbutyric acid, C4OH is hydroxybutyl carnitine. Urinary metabolites 2,3DH2MB were measured by gas chromatography–mass spectrometry (GC–MS) and are expressed in μmol/mmol of creatinine (Cr). SCPCM and blood C4-OH levels were measured by liquid chromatography–tandem mass spectrometry (LC–MS/MS) and are expressed in μmol/L. Values outside of the normal reference range are shown with arrows.

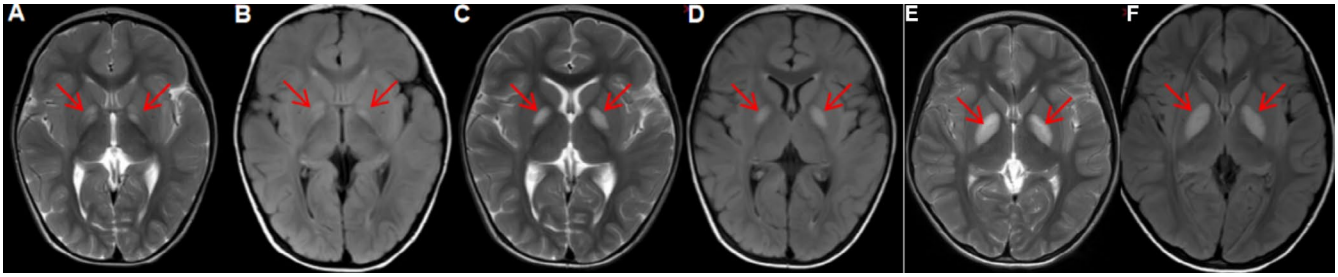

FIGURE 2 | Brain MRI images. Brain MRI of Proband 1 at 14 months old, showing bilateral symmetrical T2 and FLAIR hyperintensities in the basal ganglia (A, B) (red arrow). Brain MRI of Proband 1 at 15 months old, showing bilateral symmetrical T2 and FLAIR hyperintensities in the basal ganglia, with a slightly expanded area compared to the previous scan (C, D) (red arrow). Brain MRI of Proband 2 at 5.5 years old, showing bilateral symmetrical T2 and FLAIR hyperintensities in the globus pallidus (E, F) (red arrow).

3.2 | Clinical Findings of the Family 2

Proband 2 (Figure 1:II-4), a 6.5-year-old female, was admitted to the hospital on August 25, 2023, with a primary complaint of "fever with altered mental status for one day." The illness was characterized by fever, headache, vomiting, and drowsiness. Upon admission, a physical examination revealed a body length of 127 cm (P90) and a weight of 21.5 kg (P50). The patient was lethargic, and limb muscle strength could not be assessed due to lack of cooperation. Muscle tone was reduced, and tendon reflexes were diminished. Personal history indicated that she was the first child of a full-term natural delivery with a birth weight of 3000 g. There was no history of asphyxia or hypoxia at birth. At approximately four years of age, she developed exercise-induced dystonia in her right lower limb, characterized by painful spasms in her right foot lasting approximately 30 min. Her family history revealed that her 1-month-old sister (Figure 1:II-5) was currently healthy. The parents, who were healthy and not consanguineous, reported no family history of genetic disorders.

Auxiliary examinations, including routine blood tests, liver and kidney function tests, and assessments of electrolytes, lactate, blood ammonia, ceruloplasmin, homocysteine, and pyruvate levels, returned normal results. Cerebrospinal fluid (CSF) analysis, including cytology smear, cell count, and protein, glucose, and chloride levels, was normal, with no pathogens detected in metagenomic testing. The CO_2 binding capacity was slightly reduced at 17.2 mmol/L (normal range 22–28 mmol/L). Cardiac, abdominal, and urinary tract ultrasonography findings were unremarkable.

Blood tandem mass spectrometry showed a valine level of 175.39 umol/L (normal range 80–300 umol/L), with other values within normal limits. Urine organic acid analysis revealed elevated levels of 23DH2MB and SCPCM (Table 1). Brain MRI on August 25, 2023, demonstrated symmetrical abnormal signals with restricted diffusion in the bilateral globus pallidus (Figure 2). Following admission, the patient received fluid rehydration, mitochondrial supplementation therapy, and treatment for dystonia. Despite these interventions, the patient remained unable to walk and exhibited increased muscle tone.

3.3 | Genetic Analysis

Whole-genome sequencing identified compound heterozygous variants in the *ECHS1* gene (NM_004092) in both probands. In family 1, proband 1 and her younger sister carried the frameshift variant c.759_762del (p.Gly255Valfs*21) in exon 7 and the synonymous variant c.489G>A (p.Pro163) in exon 4. The c.759_762del variant was maternally inherited, while the c.489G>A variant was inherited from the father. The older brother of proband 1 was found to be wild-type for both *ECHS1* variants (Figure 3). In family 2, proband 2 carried two missense variants: c.518C>T (p.Ala173Val) in exon 5 and c.244G>A (p.Val82Met) in exon 2. These variants were inherited from her unaffected parents (Figure 3). No additional significant genetic variations consistent with disease phenotypes were identified in either proband.

The c.759_762del variant, which results in a glycine-to-valine substitution at position 255 and causes a frameshift leading to a premature stop codon at position 274, has not been previously reported. This truncation likely leads to loss of normal function (LoF) (PVS1) (Figure 4). The variant is cataloged in the dbSNP database as rs751562208 but is absent from major population databases, including ESP, 1000 Genomes, ExAC, and gnomAD, indicating its rarity (PM2_Supporting). According to ACMG guidelines (Richards et al. 2015; Riggs et al. 2020), the c.759_762del variant is classified as likely pathogenic (PVS1+ PM2_Supporting). The synonymous variant c.489G>A (p.Pro163=) is listed in the dbSNP database as rs140410716, with frequencies of 0.0024 in 1000 Genomes and 0.001 in gnomAD (BS1). This variant has been observed in multiple patients with relevant phenotypes and *in trans* with pathogenic or likely pathogenic variants (PM3) (Table 2). RT-PCR analysis demonstrated that this variant reduces levels of normally spliced *ECHS1* mRNA, leading to nonsense-mediated decay. Western blot analysis of fibroblasts from the patient showed a significant reduction in protein levels, with only 10% of normal levels detected (PS3) (Simon et al. 2020). Despite being classified as of uncertain significance under the ACMG guidelines, this variant is listed as disease-causing (DM) in the HGMD database.

In Proband 2, the missense variant c.518C>T (p.Ala173Val) has a frequency of 0.0007 in EXAC, 0.0002 in ESP, and 0.0010 in gnomAD. The missense variant c.244G>A (p.Val82Met) is absent from ESP, 1000 Genomes, ExAC, or gnomAD databases, suggesting its rarity (PM2_Supporting). The c.518C>T variant has been identified in multiple patients with similar phenotypes and in *trans* with pathogenic or likely pathogenic variants (PM3_VeryStrong) (Table 2). Similarly, the c.244G>A variant was detected in one patient with a related phenotype and in *trans* with a pathogenic variant (PM3). Both missense variants are predicted to be harmful by bioinformatics tools, with CADD scores of 23.2 for c.518C>T and 23.4 for c.244G>A (PP3). These variants segregated with the disease in both cases and were consistent with previous reports in the literature (PP1). Based on ACMG guidelines, the c.518C>T and c.244G>A variants are classified as pathogenic. The compound heterozygous variants identified in the *ECHS1* gene in both probands align with the clinical manifestations and were confirmed as the causative factors of ECHS1D.

3.4 | Literature Review

A systemic search was conducted using the keywords "*ECHS1*" and "ECHS1D" in the CNKI, Wanfang database, and PubMed, covering the period from database inception to May 2024. This search identified seven English-language articles with comprehensive data on *ECHS1*-related variants c.489G>A (p.Pro163=) and c.518C>T (p.Ala173Val) (Abdenur et al. 2020; Bernhardt et al. 2024; Engelstad et al. 2021; Illsinger et al. 2020; Mahajan et al. 2017; Marti-Sanchez et al. 2021; Olgiati et al. 2016). Including the present study, data were gathered on 28 patients. For the c.518C>T variant, nine patients were identified, comprising five males and four females. The age of onset ranged from 6 months to 20 years, and the age of diagnosis ranged from 4 to 22 years. Five patients presented

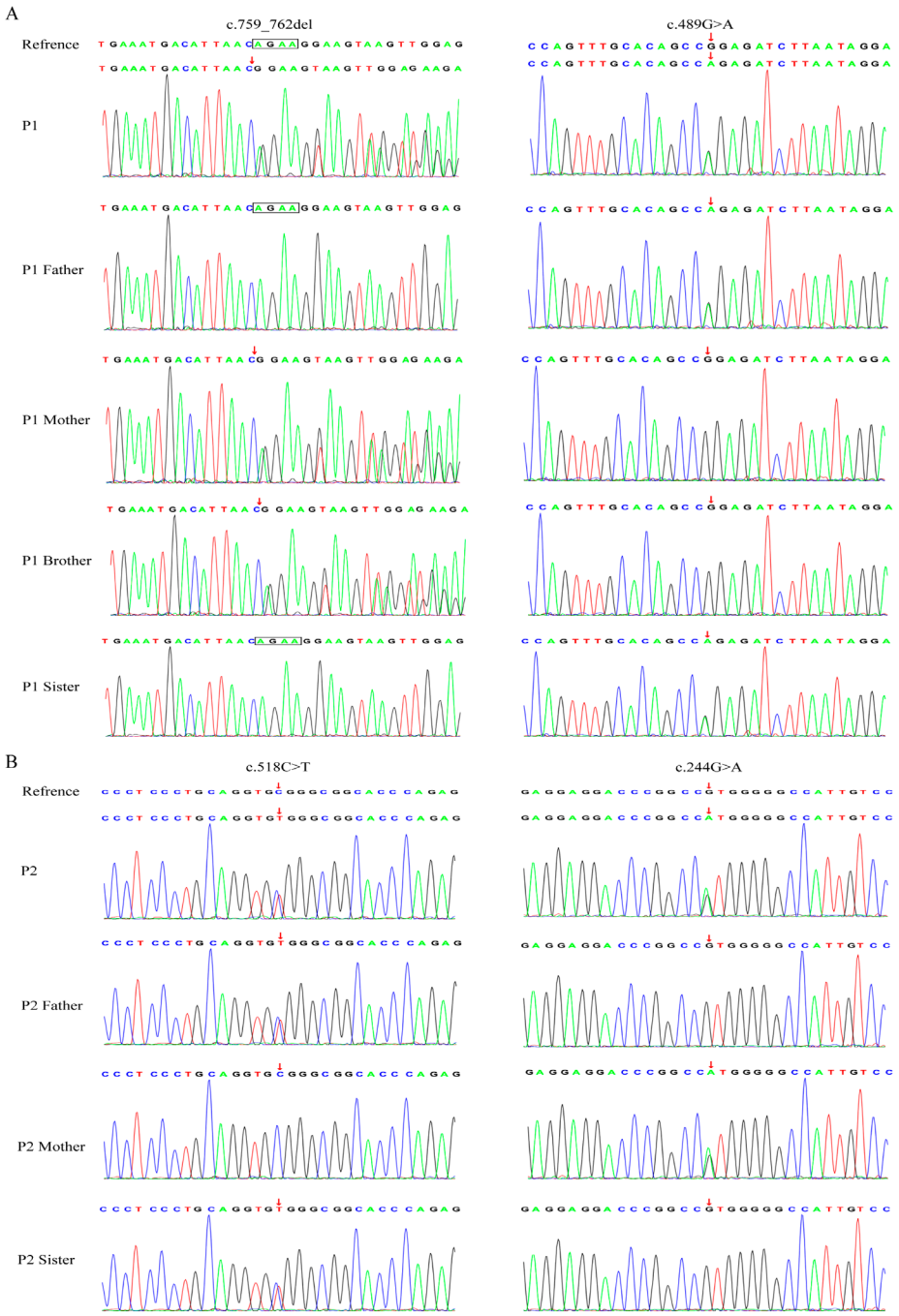

FIGURE 3 | *ECHS1* gene sequencing diagram. (A) Proband 1 and her sister carry compound heterozygous variants in the *ECHS1* gene: c.759_762del (p.Gly255Valfs*21) inherited from their mother, and c.489G>A (p.Pro163=) inherited from their father. Their brother is wild type for these variants. (B) Proband 2 has compound heterozygous variants in the *ECHS1* gene: C.518C>T (p.Ala173Val) inherited from their father, and c.244G>A (p.Val-82Met) inherited from their mother.

with paroxysmal exercise-induced dystonia triggered by infections or metabolic abnormalities, while four had feeding difficulties. Two patients exhibited intellectual disabilities. However, there were no reports of seizures, optic atrophy, hearing loss, or nystagmus. MRI scans in all patients showed symmetrical long T2 signals in the bilateral globus pallidus, with no significant increases in blood lactate levels. Elevated levels of 2,3DH2MB were detected in the urine of both patients. Importantly, no fatalities were reported in this group.

For the c.489G>A variant, data from 19 patients were reviewed, including five males, six females, and eight with unspecified sex. The age of onset ranged from 5 to 15 months, and the age of diagnosis ranged from 5 months to 47 years. Four patients experienced paroxysmal exercise-induced dystonia, and four presented with metabolic acidosis. Eleven cases were associated with infections or metabolic abnormalities. Eight patients had feeding difficulties, and eight exhibited intellectual disabilities. Six patients experienced optic nerve atrophy, five had hearing loss, and 11 presented with nystagmus. None of the patients

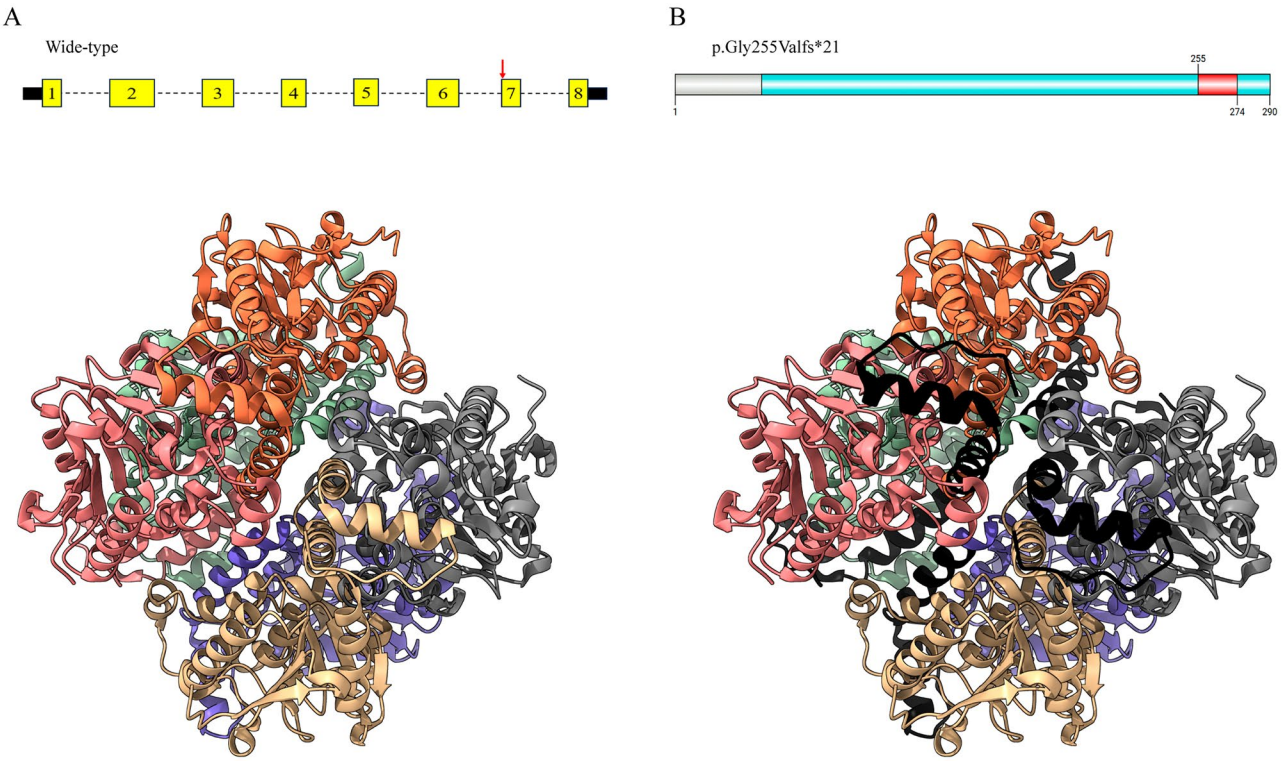

FIGURE 4 | 3D protein structure of the new *ECHS1* gene variant. The 3D structure of the wild-type ECHS1 protein (PDB ID: 2HW5) (A) and the 3D structure of the ECHS1 protein with the c.759_762del (p.Gly255Valfs*21) variant, which affects the α-helix structure and hexamer structure of ECHS1 (B, the black region of the lower section), is visualized using ChimeraX software.

reported epileptic seizures. MRI findings consistently revealed symmetrical long T2 signals in the bilateral pallidum. Elevated blood lactate levels were noted in one patient, while increased urine 2,3DH2MB were reported in four patients. Unfortunately, one patient with early onset symptoms during infancy succumbed to the disease.

4 | Discussion

This study presents the clinical and genetic characteristics of two families affected by ECHS1D, a rare mitochondrial disorder caused by variations in the *ECHS1* gene. ECHS1D is associated with a wide spectrum of clinical manifestations, including intellectual disabilities, muscle hypotonia, feeding difficulties, mitochondrial encephalopathy, hypotension, sensorineural hearing loss, seizures, optic atrophy, cardiomyopathy, respiratory insufficiency, pulmonary hypertension, hepatomegaly, steatosis, and skin laxity (Ferdinandusse et al. 2015; Fitzsimons et al. 2018; Haack et al. 2015). Based on the age of onset and clinical presentation, ECHS1D is classified into four types (Kuwajima et al. 2021): (1) Neonatal onset type: This form presents acutely with severe systemic involvement, often leading to rapid mortality. (2) Infancy-onset type: Typically occurring between 2 and 6 months of age, this subtype features developmental delays, muscular hypotonia, optic atrophy, and hearing loss. Infections exacerbate symptoms, resulting in feeding difficulties and, in some cases, seizures. (3) Slowly progressive young childhood type: Manifesting between 6 months and 3 years of age, this form primarily affects the basal ganglia and progresses slowly, allowing patients to survive into adulthood. (4) Paroxysmal exercise-induced dystonia: Onset occurs after 3 years of age with no significant neurological abnormalities between episodes. Episodes are usually triggered by exercise.

In this study, Proband 1 developed symptoms of developmental delay at 15 months of age, which progressed to metabolic acidosis. Brain MRI revealed symmetrical abnormal signals in the bilateral basal ganglia, and urine analysis indicated a metabolic disorder involving methacrylic coenzyme A. These findings are consistent with the slowly progressive young childhood type of ECHS1D. Movement disorders such as dystonia, chorea, tremor, myoclonus, Parkinsonism, and athetosis are frequently observed in ECHS1D, with dystonia being the most prevalent (François-Heude et al. 2022). Proband 2 exhibited paroxysmal exercise-induced dystonia starting at 4 years of age, which worsened significantly during infections and eventually progressed to permanent dystonia. Brain MRI revealed abnormal signals in the bilateral globus pallidus, and urine metabolite analysis confirmed a methacryloyl-CoA metabolic disorder, consistent with ECHS1D. These findings align with reports by Olgiati et al. (2016), which indicate that paroxysmal dystonia typically begins in late childhood. This study underscores the complexity and heterogeneity of ECHS1D, emphasizing the importance of detailed clinical and genetic assessments for accurate diagnosis and management.

ECHS1D was first linked to increased excretion of SCPCM and Leigh syndrome (LS) in 2014 and was identified as a distinct disease entity in 2015. Leigh syndrome, a common mitochondrial disorder in children, is also known as subacute

TABLE 2 | Clinical phenotypic, imaging, and metabolic characteristics of ECHS1D patients associated with *ECHS1* c.489G>A or c.518C>T variants.

Patient	Variant	Protein change	Sex	Onset (month)	Diagnosis (year)	First symptom	Feeding difficulties	Outcome (year)	MA	ID	Hearing loss	Optic atrophy	Nystagmus	Brain T2 hyperintense	Cerebromalacia	Encephalanalosis	White matter	Lactate	2,3DH2MB	Ala
No 1 Proband 2	c.518C>T/c.244G>A	p.A173V/p.V82M	W	48	6	PED	+	Survival 7	+	+	−	−	−	Globus pallidus	−	−	−	N	↑	N
No 2 (Marti-Sanchez et al. 2021)	c.518C>T/c.367C>T	p.A173V/p.L123P	M	18	N/A	PED	+	Survival 3	+	−	−	−	−	Globus pallidus	Globus pallidus	−	−	N	N	N
No 3 (Olgiati et al. 2016)	c.518C>T/c.232G>T	p.A173V/p.E78*	M	42	N/A	leigh-like	+	Survival 17	+	−	−	−	−	Globus pallidus, substantia nigra	−	−	−	N	N	N
No 4 (Olgiati et al. 2016)	c.518C>T/c.232G>T	p.A173V/p.E78*	M	54	N/A	PED	−	Survival 15	−	−	−	−	−	Globus pallidus	−	−	−	N	N	N
No 5 (Mahajan et al. 2017)	c.518C>T/c.817A>G	p.A173V/p.K273E	M	96	8	PED	−	Survival 8	N/A	N/A	−	−	−	Globus pallidus	−	−	−	N	N/A	N/A
No 6 (Engelstad et al. 2021)	c.518C>T/c.523G>A	p.A173V/p.G175S	W	6	N/A	leigh-like	+	Survival 6.9	−	+	N/A	N/A	N/A	Globus pallidus	−	+	+	N/A	N/A	N/A
No 7 (Illsinger et al. 2020)	c.518C>T/c.394G>A	p.A173V/p.A132T	W	30	4.75	PED	−	Survival 10.5	−	−	−	−	−	Globus pallidus	−	−	−	N	N	↑
No 8 (Illsinger et al. 2020)	c.518C>T/c.394G>A	p.A173V/p.A132T	W	20	4	MA	−	Survival 8.8	+	−	−	−	−	Globus pallidus	−	−	−	N	↑	N
No 9 (Illsinger et al. 2020)	c.518C>T/c.817A>G	p.A173V/p.K273E	M	240	22	Dysmyotonia	−	Survival 23	+	−	−	−	−	Globus pallidus middle brain	−	−	−	N	N	N
No 10 Proband 1	c.489G>A/c.759_762del	p.P163=/p.G255Vfs*21	W	15	1.5	MA	+	Survival 2	+	+	−	−	−	Globus pallidus	−	−	−	N	↑	N
No 11 P1 sister	c.489G>A/c.759_762del	p.P163=/p.G255Vfs*21	W	5	0.4	hypotonia	+	Survival 0.8	N/A	N/A	−	−	−	Globus pallidus	−	−	−	N	N/A	N
No 12 (Bernhardt et al. 2024)	c.489G>A/c.817A>G	p.P163=/p.L273G	N/A	N/A	6	PED	−	Survival 8	+	+	+	+	+	Globus pallidus	N/A	N/A	N/A	N/A	N/A	N/A
No 13 (Bernhardt et al. 2024)	c.489G>A/c.833C>T	p.P163=/p.A278V	N/A	N/A	1.6	N/A	−	Survival 3	+	−	−	−	−	Globus pallidus	N/A	N/A	N/A	N/A	N/A	N/A
No 14 (Bernhardt et al. 2024)	c.489G>A/c.299T>C	p.P163=/p.I100T	N/A	N/A	13	PED	−	Survival 14	+	+	−	+	+	Globus pallidus	N/A	N/A	N/A	N/A	N/A	N/A

(Continues)

TABLE 2 | (Continued)

Patient	Variant	Protein change	Sex	Onset (month)	Diagnosis (year)	First symptom	Feeding difficulties	Outcome (year)	MA	ID	Hearing loss	Optic atrophy	Nystagmus	Brain T2 hyperintense	Cerebromalacia	Encephalanalosis	White matter	Lactate	2,3DH2MB	Ala
No 15 (Bernhardt et al. 2024)	c.489G>A/c.607G>A	p.P163=/p.A203T	N/A	N/A	8	PED	−	Survival 10	+	−	−	−	+	Globus pallidus	N/A	N/A	N/A	N/A	N/A	N/A
No 16 (Bernhardt et al. 2024)	c.489G>A/c.299T>C	p.P163=/p.I100T	N/A	N/A	30	N/A	−	Survival 31	+	+	−	+	−	Globus pallidus	N/A	N/A	N/A	N/A	N/A	N/A
No 17 (Bernhardt et al. 2024)	c.489G>A/c.744T>G	p.P163=/p.P248L	N/A	N/A	N/A	N/A	−	N/A	+	−	−	+	−	Globus pallidus	N/A	N/A	N/A	N/A	N/A	N/A
No 18 (Bernhardt et al. 2024)	c.489G>A/c.817A>G	p.P163=/p.L273G	M	N/A	26	N/A	+	Survival 27	−	+	+	+	−	Globus pallidus	N/A	N/A	N/A	N/A	N/A	N/A
No 19 (Bernhardt et al. 2024)	c.489G>A/c.817A>G	p.P163=/p.L273G	W	N/A	47	N/A	+	Survival 48	−	+	+	+	−	Globus pallidus	N/A	N/A	N/A	N/A	N/A	N/A
No 20 (Bernhardt et al. 2024)	c.489G>A/c.299T>C	p.P163=/p.I100T	W	N/A	5	PED	N/A	Survival 6	+	−	+	+	+	Globus pallidus	N/A	N/A	N/A	N/A	N/A	N/A
No 21 (Bernhardt et al. 2024)	c.489G>A/c.299T>C	p.P163=/p.I100T	W	N/A	1.3	N/A	N/A	Survival 2	+	−	−	−	+	Globus pallidus	N/A	N/A	N/A	N/A	N/A	N/A
No 22 (Bernhardt et al. 2024)	c.489G>A/c.299T>C	p.P163=/p.I100T	M	N/A	On birth	N/A	N/A	Survival 0.6	−	−	−	−	+	N/A	N/A	N/A	N/A	N/A	N/A	N/A
No 23 (Bernhardt et al. 2024)	c.489G>A/c.817A>G	p.P163=/p.L273G	N/A	N/A	28	N/A	N/A	Survival 29	−	−	+	+	+	Globus pallidus	N/A	N/A	N/A	N/A	N/A	N/A
No 24 (Bernhardt et al. 2024)	c.489G>A/c.827T>C	p.P163=/p.M276T	N/A	N/A	2	N/A	N/A	Survival 2	+	−	−	+	−	Globus pallidus	N/A	N/A	N/A	N/A	N/A	N/A
No 25 (Abdenur et al. 2020)	c.489G>A/c.832G>A	p.P163=/p.A278T	M	6	13	MA	+	Survival 13.8	N/A	+	−	+	+	Globus pallidus	Basal section	+	+	N	↑	N
No 26 (Abdenur et al. 2020)	c.489G>A/c.832G>A	p.P163=/p.A278T	M	infancy	N/A	MA	+	Death 9	N/A	+	−	+	+	Globus pallidus	Basal section	+	+	N	↑	N
No 27 (Abdenur et al. 2020)	c.489G>A/c.832G>A	p.P163=/p.A278T	M	15	6	MA	+	Survival 6.3	N/A	+	−	+	+	Balbus pallidum, Caudate nucleus head	Basal section	+	+	N	↑	N
No 28 (Abdenur et al. 2020)	c.489G>A/c.832G>A	p.P163=/p.A278T	W	8	8	Developmental backwardness	+	Survival 8	+	+	−	−	+	Globus pallidus	Basal section	+	+	↑	N	N

Abbreviations: ↑, increased value; ID, intellectual disability; M, Man; MA, metabolic acidosis; *N*, normal; N/A, not available; PED, Paroxysmal exercise induced dystonia; W, Woman.

necrotizing encephalomyopathy. This neurodegenerative condition is genetically heterogeneous and linked to mutations in over 75 genes. Its pathogenesis is primarily associated with mitochondrial dysfunction. Mitochondrial diseases are relatively rare and present with diverse symptoms, which can delay diagnosis. Children with developmental delay, hypotonia, abnormal eye development, gastrointestinal dysfunction, and no clear genetic diagnosis should undergo regular re-evaluation, with particular attention to blood lactate and ammonia levels. Patients with ECHS1D often exhibit elevated lactic acid levels, moderate hyperammonemia, and increased organic acid levels in blood and urine (Ganetzky et al. 2016). Although lactate levels are nonspecific, the detection of 2-methyl-2,3dihydroxy butyrate and its metabolites in urine provides a more specific diagnostic marker (Kuwajima et al. 2021; Peters et al. 2015). In this study, both probands exhibited elevated urinary levels of 2-methyl-2,3dihydroxybutyric acid, underscoring its potential as a critical diagnostic indicator for ECHS1D. This condition leads to the accumulation of methacryloyl-coenzyme A and acryloyl-CoA, which causes brain cell damage. Brain MRI findings typically include symmetrical T2 hyperintensities in the caudate nucleus, putamen, and globus pallidus, consistent with Leigh syndrome (Yamada et al. 2015). Given the clinical and imaging overlaps between ECHS1D and Leigh syndrome, timely genetic testing and metabolite analysis are essential for accurate diagnosis and effective management of affected patients.

The *ECHS1* gene is located in the chromosomal region 10q26.2-q26.3 and contains eight exons. It is widely expressed in various tissues. The encoded precursor protein comprises 290 amino acids and is processed in the mitochondria to form the mature 28.3 kDa ECHS1 protein, which assembles into a "dimer trimer" structure of a homologous hexamer (Sharpe and McKenzie 2018). The ECHS1 protein functions as a crotonase, catalyzing the second step of mitochondrial fatty acid β-oxidation (FAO) by converting C4-C6 fatty acyl-CoA to β-hydroxyacyl-CoA. Moreover, *ECHS1* plays a role in valine and isoleucine catabolism, converting methacryloyl-CoA to 3-hydroxyisobutyryl-CoA and acrylyl-CoA to 3-hydroxypropionoyl-CoA. *ECHS1* deficiency leads to the accumulation of toxic metabolites, impairing mitochondrial oxidative phosphorylation and energy production, thereby causing various clinical symptoms (Fitzsimons et al. 2018). As of January 2025, the HGMD included 93 *ECHS1* variants, primarily missense variants, along with splicing, insertion, and deletion variants. Most variants are compound heterozygous and do not cluster as significant hotspot mutations. While all genotypes reduce *ECHS1* function, the severity of pathogenicity varies widely.

For instance, the p.Asn59Ser variant is associated with high lethality in some patients, whereas the p.Ala173Val variant is linked to milder symptoms, highlighting the clinical heterogeneity of ECHS1D. The p.Ala173Val variant, located near an exon-intron boundary, replaces a highly conserved amino acid, potentially disrupting mRNA splicing. Clinically, this variant presents with dystonia, mitochondrial encephalopathy, and brain white matter degeneration but manifests predominantly as paroxysmal dystonia. Symptoms typically occur at approximately 3.4 years of age and are triggered by prolonged exercise, fasting, or fever, with normal neurological function between episodes (Burgin and McKenzie 2020).

In this study, Proband 2 developed postexercise unilateral lower limb dystonia at 4 years of age, which initially resolved spontaneously within minutes. However, following a febrile episode, the proband experienced acute encephalopathy and persistent dystonia. This phenomenon has been reported previously, suggesting that increased energy demand may trigger paroxysmal dystonia, potentially indicating ECHS1D (Olgiati et al. 2016). Despite undergoing rehydration, mitochondrial replacement therapy, and dystonia management, the patient remained unable to ambulate and exhibited increased muscle tone. Common imaging findings in mitochondrial disorders include white matter demyelination, brain atrophy, ventricular dilatation, and thinning of the corpus callosum (Bonfante et al. 2016). However, carriers of the p.Ala173Val variant typically do not exhibit such abnormalities, whereas carriers of the p.Pro163 variant often exhibit brain atrophy and white matter abnormalities. The p.Pro163 variant, first identified in 2020 in four ECHS1D patients, has a high carrier frequency and is often overlooked in routine genomic testing. Homozygous carriers of this variant generally exhibit mild phenotypes, though detailed long-term effects remain underreported. This discrepancy may explain the high carrier frequency of the variant relative to the lower incidence of ECHS1D.

Patients with compound heterozygous variants, such as p.Pro163 and p.Ala278Thr, often have poorer prognoses, presenting with metabolic acidosis, acute encephalopathy, and extensive basal ganglia lesions on imaging (Abdenur et al. 2020). In this study, proband 1 carried a compound heterozygous variation of p.Pro163 and c.759_762del, presenting with metabolic acidosis and developmental delay. The newly identified c.759_762del variant, which causes a frameshift, may be associated with metabolic acidosis and acute encephalopathy. This finding expands the known spectrum of *ECHS1* variations and highlights the complex pathogenic mechanisms underlying ECHS1D.

Although no specific treatment exists for ECHS1D, symptoms can be alleviated and quality of life improved through dietary management, drug therapy, and comprehensive treatment strategies. Mitochondrial vitamin supplement therapy, which combines multiple vitamins and coenzymes to enhance mitochondrial function, has demonstrated limited and inconsistent clinical efficacy, requiring further validation and optimization. The ketogenic diet—a high-fat, low-carbohydrate regimen—offers an alternative energy source while reducing the production of toxic metabolites from sugar and protein catabolism. Additionally, this diet improves antioxidant activity and mitigates cellular damage caused by reactive oxygen species (ROS), making it a promising therapeutic option for ECHS1D (Gano et al. 2014).

A low-protein diet may help reduce the accumulation of toxic metabolites and potentially slow disease progression. Restricted valine intake has been reported to improve clinical symptoms, biochemical markers, and imaging findings (Stenton et al. 2022). Valine intake should follow established guidelines for managing metabolic disorders such as maple syrup urine disease (MSUD),

propionic acidemia (PA), and methylmalonic acidemia (MMA) to prevent excessive metabolite accumulation. The antioxidant N-acetylcysteine (NAC) replenishes neuronal glutathione stores and protects nerve cells from oxidative damage. Combination therapy incorporating NAC and other agents may enhance therapeutic efficacy and positively impact clinical symptoms (Stenton et al. 2022). Tricarboxylic acid (TCA), an energy metabolism enhancer, has been shown to alleviate energy deficiency symptoms by increasing energy production through the TCA cycle in ECHS1D patients (Engelstad et al. 2021). Additionally, physical exercise and physiotherapy can improve mitochondrial function and overall patient outcomes.

Certain medications, including valproic acid, topiramate, statins, aminoglycosides, erythromycin, and acetaminophen, may exacerbate ECHS1D symptoms and should be avoided. Viral infections, as observed in the two probands in this study, can significantly worsen symptoms. Therefore, it is imperative to closely monitor the status of vaccinated children during routine immunization against infectious diseases in order to prevent potential complications arising from infections and mitigate the risk of symptom exacerbation. Despite interventions such as acid rehydration, mitochondrial supplement therapy, and other treatments, the clinical symptoms of both probands in this study showed limited improvement. This underscores that while comprehensive treatment can alleviate certain symptoms, current therapeutic options remain insufficient for addressing severe manifestations of ECHS1D. Future research should focus on developing novel therapeutic strategies, including precise regulation of mitochondrial function, gene repair techniques, and interventions targeting specific metabolic pathways.

5 | Conclusions

This study examined two families affected by ECHS1D and highlighted the clinical diversity and complexity associated with *ECHS1* variants. Previous studies have shown that ECHS1D typically manifests early, progresses rapidly, and is associated with high disability and mortality rates. Patients often present with severe symptoms such as intellectual disabilities, hypotonia, and metabolic disorders, resulting in a poor prognosis. However, patients whose primary symptom is paroxysmal exercise-induced dystonia (PED) generally have a milder condition and a better prognosis. Furthermore, a subset of patients experienced disease onset during adulthood. These observations highlight the clinical variability of ECHS1D, which manifests not only in differing presentations and severities but also in age at onset. Likewise, significant variations in disease severity and outcomes are contingent upon the specific phenotype. In clinical practice, ECHS1D should be considered in patients presenting with unexplained PED, and genetic testing should be conducted for early diagnosis. For patients diagnosed with ECHS1D, early interventions—including nutritional support, vitamin therapy, a low-protein diet, and antioxidant treatment—may help slow disease progression and enhance quality of life. Future research should focus on validating the functional impact of novel *ECHS1* variants, conducting longitudinal studies to assess long-term outcomes, and exploring the genetic diversity of ECHS1D in larger and more diverse populations. These efforts may ultimately lead to improved diagnostic algorithms and the development of targeted therapeutic strategies for this rare but complex disorder.

Author Contributions

Jihua Wu and Bin Yang: designed the study. **Jihua Wu:** wrote the manuscript. **Bin Yang:** revised the article. **Jihua Wu, Xuehui Hu, Zhongli Zhao, and Zhen Zhao:** collecting and analyzing data. All authors contributed to the article and approved the submitted version.

Acknowledgments

We thank the affected individuals and their family members for participating in this study.

Conflicts of Interest

The authors declare no conflicts of interest.

Data Availability Statement

All data generated or analyzed during this study are included in this published article. The original contributions presented in this study are publicly available. The *ECHS1* variants NM_004092.3: c.759_762del and c.489G>A, c.518C>T, and c.244G>A were submitted to the LSDB (http://www.lovd.nl):https://databases.lovd.nl/shared/variants/0000987896#00006849, https://databases.lovd.nl/shared/variants/0000987896#00006849, https://databases.lovd.nl/shared/variants/0000987898#00006849, https://databases.lovd.nl/shared/variants/0000987899#00006849.

References

Abdenur, J. E., M. Sowa, M. Simon, et al. 2020. "Medical Nutrition Therapy in Patients With HIBCH and ECHS1 Defects: Clinical and Biochemical Response to Low Valine Diet." *Molecular Genetics and Metabolism Reports* 24: 100617. https://doi.org/10.1016/j.ymgmr.2020.100617.

Balasubramaniam, S., L. G. Riley, D. Bratkovic, et al. 2017. "Unique Presentation of Cutis Laxa With Leigh-Like Syndrome due to ECHS1 Deficiency." *Journal of Inherited Metabolic Disease* 40, no. 5: 745–747. https://doi.org/10.1007/s10545-017-0036-4.

Bernhardt, I., L. E. Frajman, B. Ryder, et al. 2024. "Further Delineation of Short-Chain Enoyl-CoA Hydratase Deficiency in the Pacific Population." *Molecular Genetics and Metabolism* 142, no. 3: 108508. https://doi.org/10.1016/j.ymgme.2024.108508.

Bonfante, E., M. K. Koenig, R. B. Adejumo, V. Perinjelil, and R. F. Riascos. 2016. "The Neuroimaging of Leigh Syndrome: Case Series and Review of the Literature." *Pediatric Radiology* 46, no. 4: 443–451. https://doi.org/10.1007/s00247-015-3523-5.

Burgin, H., A. J. Sharpe, S. Nie, et al. 2023. "Loss of Mitochondrial Fatty Acid β-Oxidation Protein Short-Chain Enoyl-CoA Hydratase Disrupts Oxidative Phosphorylation Protein Complex Stability and Function." *FEBS Journal* 290, no. 1: 225–246. https://doi.org/10.1111/febs.16595.

Burgin, H. J., and M. McKenzie. 2020. "Understanding the Role of OXPHOS Dysfunction in the Pathogenesis of ECHS1 Deficiency." *FEBS Letters* 594, no. 4: 590–610. https://doi.org/10.1002/1873-3468.13735.

Engelstad, K., R. Salazar, D. Koenigsberger, et al. 2021. "Exploring Triheptanoin as Treatment for Short Chain Enoyl CoA Hydratase Deficiency." *Annals of Clinical Translational Neurology* 8, no. 5: 1151–1157. https://doi.org/10.1002/acn3.51359.

Ferdinandusse, S., M. W. Friederich, A. Burlina, et al. 2015. "Clinical and Biochemical Characterization of Four Patients With Mutations in ECHS1." *Orphanet Journal of Rare Diseases* 10: 79. https://doi.org/10.1186/s13023-015-0290-1.

Fitzsimons, P. E., C. L. Alston, P. E. Bonnen, et al. 2018. "Clinical, Biochemical, and Genetic Features of Four Patients With Short-Chain Enoyl-CoA Hydratase (ECHS1) Deficiency." *American Journal of Medical Genetics. Part A* 176, no. 5: 1115–1127. https://doi.org/10.1002/ajmg.a.38658.

François-Heude, M. C., E. Lebigot, E. Roze, et al. 2022. "Movement Disorders in Valine Métabolism Diseases Caused by HIBCH and ECHS1 Deficiencies." *European Journal of Neurology* 29, no. 11: 3229–3242. https://doi.org/10.1111/ene.15515.

Ganetzky, R. D., K. Bloom, R. Ahrens-Nicklas, et al. 2016. "ECHS1 Deficiency as a Cause of Severe Neonatal Lactic Acidosis." *JIMD Reports* 30: 33–37. https://doi.org/10.1007/8904_2016_538.

Gano, L. B., M. Patel, and J. M. Rho. 2014. "Ketogenic Diets, Mitochondria, and Neurological Diseases." *Journal of Lipid Research* 55, no. 11: 2211–2228. https://doi.org/10.1194/jlr.R048975.

Haack, T. B., C. B. Jackson, K. Murayama, et al. 2015. "Deficiency of ECHS1 Causes Mitochondrial Encephalopathy With Cardiac Involvement." *Annals of Clinical Translational Neurology* 2, no. 5: 492–509. https://doi.org/10.1002/acn3.189.

Illsinger, S., G. C. Korenke, S. Boesch, et al. 2020. "Paroxysmal and Non-Paroxysmal Dystonia in 3 Patients With Biallelic ECHS1 Variants: Expanding the Neurological Spectrum and Therapeutic Approaches." *European Journal of Medical Genetics* 63, no. 11: 104046. https://doi.org/10.1016/j.ejmg.2020.104046.

Kuwajima, M., K. Kojima, H. Osaka, et al. 2021. "Valine Metabolites Analysis in ECHS1 Deficiency." *Molecular Genetics and Metabolism Reports* 29: 100809. https://doi.org/10.1016/j.ymgmr.2021.100809.

Mahajan, A., J. Constantinou, and C. Sidiropoulos. 2017. "ECHS1 Deficiency-Associated Paroxysmal Exercise-Induced Dyskinesias: Case Presentation and Initial Benefit of Intervention." *Journal of Neurology* 264, no. 1: 185–187. https://doi.org/10.1007/s00415-016-8381-z.

Marti-Sanchez, L., H. Baide-Mairena, A. Marcé-Grau, et al. 2021. "Delineating the Neurological Phenotype in Children With Defects in the ECHS1 or HIBCH Gene." *Journal of Inherited Metabolic Disease* 44, no. 2: 401–414. https://doi.org/10.1002/jimd.12288.

Olgiati, S., M. Skorvanek, M. Quadri, et al. 2016. "Paroxysmal Exercise-Induced Dystonia Within the Phenotypic Spectrum of ECHS1 Deficiency." *Movement Disorders* 31, no. 7: 1041–1048. https://doi.org/10.1002/mds.26610.

Peters, H., N. Buck, R. Wanders, et al. 2014. "ECHS1 Mutations in Leigh Disease: A New Inborn Error of Metabolism Affecting Valine Metabolism." *Brain* 137, no. Pt 11: 2903–2908. https://doi.org/10.1093/brain/awu216.

Peters, H., S. Ferdinandusse, J. P. Ruiter, R. J. Wanders, A. Boneh, and J. Pitt. 2015. "Metabolite Studies in HIBCH and ECHS1 Defects: Implications for Screening." *Molecular Genetics and Metabolism* 115, no. 4: 168–173. https://doi.org/10.1016/j.ymgme.2015.06.008.

Richards, S., N. Aziz, S. Bale, et al. 2015. "Standards and guidelines for the interpretation of sequence variants: a joint consensus recommendation of the American College of Medical Genetics and Genomics and the Association for Molecular Pathology." *Genetics in Medicine* 17, no. 5: 405–424. https://doi.org/10.1038/gim.2015.30.

Riggs, E. R., E. F. Andersen, A. M. Cherry, et al. 2020. "Technical Standards for the Interpretation and Reporting of Constitutional Copy-Number Variants: A Joint Consensus Recommendation of the American College of Medical Genetics and Genomics (ACMG) and the Clinical Genome Resource (ClinGen)." *Genetics in Medicine* 22, no. 2: 245–257. https://doi.org/10.1038/s41436-019-0686-8.

Sharpe, A. J., and M. McKenzie. 2018. "Mitochondrial Fatty Acid Oxidation Disorders Associated With Short-Chain Enoyl-CoA Hydratase (ECHS1) Deficiency." *Cells* 7, no. 6: 46. https://doi.org/10.3390/cells7060046.

Simon, M. T., S. S. Eftekharian, S. Ferdinandusse, et al. 2020. "ECHS1 Disease in Two Unrelated Families of Samoan Descent: Common Variant – Rare Disorder." *American Journal of Medical Genetics Part A* 185, no. 1: 157–167. https://doi.org/10.1002/ajmg.a.61936.

Stenton, S. L., Y. Zou, H. Cheng, et al. 2022. "Leigh Syndrome: A Study of 209 Patients at the Beijing Children's Hospital." *Annals of Neurology* 91, no. 4: 466–482. https://doi.org/10.1002/ana.26313.

Yamada, K., K. Aiba, Y. Kitaura, et al. 2015. "Clinical, Biochemical and Metabolic Characterisation of a Mild Form of Human Short-Chain Enoyl-CoA Hydratase Deficiency: Significance of Increased N-Acetyl-S-(2-Carboxypropyl)cysteine Excretion." *Journal of Medical Genetics* 52, no. 10: 691–698. https://doi.org/10.1136/jmedgenet-2015-103231.

Yang, Z., J. Cao, Y. Song, et al. 2022. "Whole-Exome Sequencing Identified Novel Variants in Three Chinese Leigh Syndrome Pedigrees." *American Journal of Medical Genetics. Part A* 188, no. 4: 1214–1225. https://doi.org/10.1002/ajmg.a.62641.

Supporting Information

Additional supporting information can be found online in the Supporting Information section.